O-516

J. Chem. Thermodynamics **1993**, 25, 1391–1401

Thermodynamic properties of silicides

II. Heat capacity at temperatures T from 5.9 K to 341 K and derived thermodynamic properties to $T = 1200$ K of tungsten disilicide: $WSi_{2.06}$

Jane E. Callanan,

Callanan Associates, 2888 Bluff, Suite 429, Boulder, CO 80301, U.S.A.

Ron D. Weir,[a]

Department of Chemistry and Chemical Engineering, Royal Military College of Canada, Kingston, Ontario K7K 5L0, Canada

and Edgar F. Westrum, Jr.

Department of Chemistry, University of Michigan, Ann Arbor, MI 48109-1055, U.S.A.

(Received 2 March 1993; in final form 2 June 1993)

The heat capacity of tungsten disilicide $WSi_{2.06}$ was measured over the temperature range $5.9 < (T/K) < 341$ using adiabatic calorimetry. Our results show that neither a phase transition nor anomalies are present. A contribution from the electronic molar heat capacity is present and $\gamma = (1.33 \pm 0.25)\ mJ \cdot K^{-2} \cdot mol^{-1}$. For the lattice, the Debye characteristic temperature $\Theta_D^C = (317.8 \pm 3.3)$ K. From our results, the standard molar entropy $S_m^\circ(WSi_{2.06}, cr, 298.15\ K) = (68.43 \pm 0.17)\ J \cdot K^{-1} \cdot mol^{-1}$. On the basis of this result, the standard molar Gibbs free energy of formation $\Delta_f G_m^\circ(WSi_{2.06}, cr, 298.15\ K) = -(79.5 \pm 5.5)\ kJ \cdot mol^{-1}$. Heat capacities derived from drop calorimetry at $T = 460$ K together with those reported in this work allowed standard molar thermodynamic functions to be presented at selected temperatures from 5 K to 1200 K.

1. Introduction

The transition-metal silicides, like the transition-metal dichalcogenides, possess special properties that lend themselves to applications as engineering materials. The well defined family of compounds M_aSi_b contains the metal element M within groups 13 through 18. Their stability, resistance to oxidation, low electrical resistivity, and great tensile strength at high temperatures naturally lead to their use in high-temperature furnaces and coatings, integrated circuits, and ceramic reinforcements in metal matrices and other composites.[1,2] Tungsten disilicide WSi_2 is especially suitable as a refractory material.[3–5] The need to know its thermodynamic properties

[a] To whom correspondence should be sent.

0021-9614/93/111391+11 $08.00/0

has prompted several studies to obtain key values such as the standard molar enthalpy of formation,[6-9] enthalpy increments at high temperatures,[10,11] and the energy of combustion.[12]

In the stable form at room temperature, tungsten disilicide is tetragonal with space group I4/mmm of No. 139 D_{4h}^{17}, lattice parameters: $a = 0.3212$ nm, $c = 0.7880$ nm, and $Z = 2$.[13] The absence of low-temperature thermodynamic quantities in general, and heat capacity, enthalpy increments, and standard entropy in particular, led us to investigate these properties as part of our experimental programme on advanced materials. In this paper, we report for the first time the results of adiabatic heat-capacity measurements on WSi_2 at any temperature.

2. Experimental

The sample of WSi_2 was a gift from Dr M. Sugano, Nippon Mining Company, Japan, and is from the same batch used in the combustion studies at the National Institute of Standards and Technology (NIST).[12] The formula of the specimen is taken to be $WSi_{2.060\pm0.002}$. The WSi_2 had been prepared by heating a mixture of tungsten and silicon in an evacuated tube (pressure $p = 1$ mPa), initially at temperature $T = 1073$ K to $T = 1573$ K, and then at $T = 1553$ K to $T = 1773$ K. The details of the synthesis are presented in a patent.[14] The finely divided powder was shipped from NIST to the Royal Military College (RMC) where it was stored and handled, including the filling of the calorimeter vessel, within a glovebox filled with dry circulating nitrogen. When received at RMC, crystals were removed for X-ray study and the Guinier–de-Wolff diffraction pattern was in agreement with the standard pattern for WSi_2, No. 11-195 as determined by the Joint Committee for Powder Diffraction Standards. Its structure was found to be tetragonal at room temperature with parameters: $a = (0.3212 \pm 0.0001)$ nm, $c = (0.7830 \pm 0.0001)$ nm, which compare with the JCPDS 11-195: $a = 0.3211$ nm and $c = 0.7868$ nm, and with Zachariasen:[13] $a = 0.3212$ nm and $c = 0.7880$ nm.

The molar isobaric heat capacity $C_{p,m}$ was measured at temperatures from 5.9 K to 341 K by adiabatic calorimetry in the Mark XIII adiabatic cryostat, which is an upgraded version of the Mark II cryostat described previously.[15] A guard shield was incorporated around the adiabatic shield. A capsule-type platinum resistance thermometer (laboratory designation A-5) was used for the temperature measurements. The thermometer was calibrated at the U.S. National Bureau of Standards (N.B.S., now NIST) against the IPTS-1948 (as revised in 1960)[16] for temperatures above 90 K, against the 1955 N.B.S. (NIST) provisional scale from $T = 10$ K to $T = 90$ K, and by the technique of McCrackin and Chang[17] at $T < 10$ K. These calibrations are judged to reproduce thermodynamic temperatures to within 0.03 K at $10 \leqslant (T/\mathrm{K}) \leqslant 90$ K and within 0.04 K at $T > 90$ K.[18] The effects of changing the temperature scale to ITS-90 vary over the range $90 \leqslant (T/\mathrm{K}) \leqslant 350$ from $0.020 \leqslant \{(T_{90} - T_{48})/\mathrm{K}\} \leqslant -0.27$, and for the range $14 \leqslant (T/\mathrm{K}) \leqslant 90$ from $-0.008 \leqslant \{(T_{90} - T_{55})/\mathrm{K}\} \leqslant 0.018$.[19,20] The changes in heat capacity, enthalpy increment, and entropy resulting from the conversion from IPTS-68 to ITS-90 have been shown for a number of materials to lie within the experimental error of the

measurements over the range from $14 \leqslant (T/\mathrm{K}) \leqslant 2150$.[20] Measurements of mass, current, potential difference, and time were based upon calibrations done at the U.S.N.B.S. (NIST). The heat capacities at temperatures from about 6 K to 329 K were acquired with the assistance of a computer,[21,22] which was programmed for a series of determinations. During the drift periods, both the calorimetric temperature and the first and second derivatives of temperature with respect to time were recorded to establish the equilibrium temperature of the calorimeter before and after the energy input. While the calorimeter heater was on, the heater current and potential difference as well as the duration of the heating interval were determined. Also recorded was the apparent heat capacity of the system, which included the calorimeter, heater, thermometer, and sample.

A gold-plated copper calorimeter (laboratory designation W-139) with four internal vertical vanes and a central entrant well for (heater + thermometer) was loaded with WSi_2. Following the loading, the calorimeter was evacuated and pumping was continued for several hours to ensure that any moisture released from the sample was removed. After addition of $p \approx 30$ kPa He(g) (at $T = 296$ K) to facilitate thermal equilibration, the vessel was then sealed by means of an annealed gold gasket tightly pressed on to the stainless-steel knife edge of the calorimeter top using a screw closure about 5 mm in diameter.

Buoyancy corrections were calculated on the basis of a crystallographic density of 9.805 $g \cdot cm^{-3}$, derived from the X-ray diffraction of our sample. The mass of WSi_2 was 25.35736 g ($\triangleq 0.1049099$ mol, based on its molar mass of 241.706 $g \cdot mol^{-1}$ as calculated from the 1985 IUPAC recommended atomic masses of the elements).[23]

The thermal history of the WSi_2 measurements is represented by the following linear array. The arrows denote either cooling or heating, which correspond to the acquisition of heat-capacity results.

$$T = 300\ \mathrm{K} \xrightarrow{10\ \mathrm{h}} 6\ \mathrm{K} \underset{\text{Series I}}{\xrightarrow{10\ \mathrm{h}}} 77\ \mathrm{K} \underset{\text{Series II}}{\xrightarrow{12\ \mathrm{h}}} 223\ \mathrm{K} \underset{\text{Series III}}{\xrightarrow{6\ \mathrm{h}}} 341\ \mathrm{K}.$$

3. Results

The experimental molar heat capacities $C_{p,\mathrm{m}}$ of our $WSi_{2.06}$ sample are listed in table 1, where the results are presented in order of increasing temperature. The measurements were made in three series that began at $T = 5.9$ K and ended at $T = 341$ K. The probable errors in heat capacity decrease from about $10^{-2} \cdot C_{p,\mathrm{m}}$ at $T = 10$ K to less than $2 \cdot 10^{-3} \cdot C_{p,\mathrm{m}}$ at temperatures above 30 K. The heat capacity of the sample varied from $0.20 \cdot C_{p,\mathrm{total}}$ at $T = 15$ K to $0.45 \cdot C_{p,\mathrm{total}}$ at $T = 325$ K where $C_{p,\mathrm{total}}$ is the total heat capacity of the sample plus the calorimeter vessel.

Shown in figure 1 is the experimental $C_{p,\mathrm{m}}/R$ (where R is the gas constant) against T plot for $WSi_{2.06}$ from $T = 5.9$ K to $T = 341$ K. The curve appears smooth and without anomalies.

The standard molar thermodynamic functions are given at selected temperatures in table 2. The heat capacities at $T \leqslant 8$ K were determined by fitting our

TABLE 1. Experimental molar heat capacity of $WSi_{2.06}$
($M = 241.706\ g \cdot mol^{-1}$, $R = 8.31451\ J \cdot K^{-1} \cdot mol^{-1}$)

T/K	$C_{p,m}/R$	T/K	$C_{p,m}/R$	T/K	$C_{p,m}/R$	T/K	$C_{p,m}/R$	T/K	$C_{p,m}/R$	T/K	$C_{p,m}/R$
6.80	0.0035	28.47	0.169	67.76	1.720	127.09	4.578	188.56	6.570	263.37	7.879
8.01	0.0050	30.38	0.207	71.58	1.909	131.17	4.726	192.72	6.656	269.50	7.961
10.44	0.0094	32.30	0.250	75.42	2.112	135.24	4.895	196.86	6.752	275.71	8.067
11.21	0.011	34.24	0.299	79.27	2.310	139.33	5.029	200.97	6.834	281.91	8.146
12.25	0.015	36.21	0.353	83.07	2.516	143.41	5.185	205.12	6.910	288.16	8.220
13.64	0.020	38.36	0.422	87.00	2.695	147.50	5.313	209.31	7.009	294.27	8.300
14.78	0.026	40.58	0.496	90.96	2.893	151.59	5.472	213.40	7.073	300.53	8.369
15.96	0.032	42.79	0.577	94.91	3.073	155.69	5.609	217.52	7.161	306.65	8.430
17.30	0.039	45.36	0.674	98.90	3.281	159.79	5.726	221.65	7.234	312.90	8.485
18.79	0.049	48.11	0.785	102.89	3.499	163.90	5.849	226.52	7.318	319.15	8.522
20.29	0.059	50.87	0.901	106.89	3.698	168.00	5.974	232.38	7.410	325.40	8.569
21.79	0.072	53.89	1.039	110.92	3.864	172.11	6.125	238.58	7.509	331.70	8.596
23.32	0.088	57.15	1.201	114.96	4.043	176.23	6.243	244.77	7.610	337.99	8.643
24.88	0.108	60.43	1.363	119.01	4.216	180.36	6.344	250.87	7.701		
26.60	0.135	63.97	1.541	123.05	4.406	184.47	6.455	257.14	7.801		

experimental values at $T \leqslant 20$ K to the limiting form of the Debye equation that included a term due to electronic conduction (see section 4). Plots of $C_{p,m}/T$ against T^2 and of $(C_{p,m} - \gamma T)/T^3$ against T^2, when extrapolated to $T \rightarrow 0$, yielded identical results.

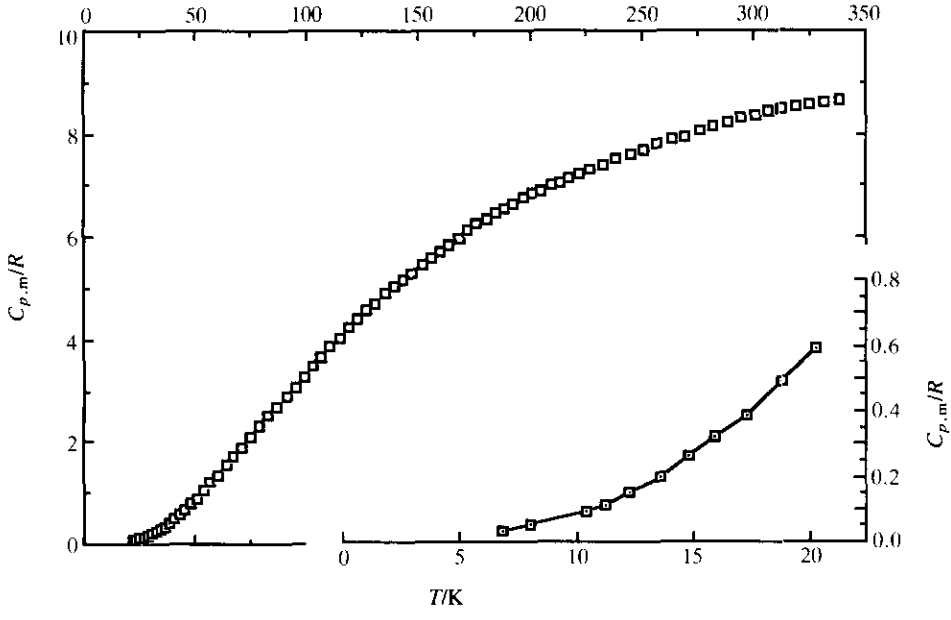

FIGURE 1. Experimental molar heat capacities $C_{p,m}$ at constant pressure plotted against temperature T for $WSi_{2.06}$. The region below $T = 22$ K is enlarged in the lower right-hand corner.

TABLE 2. Standard molar thermodynamic functions for $WSi_{2.06}$

$\{M = 241.706\ g \cdot mol^{-1}$; $p^\circ = 101.325\ kPa$; $R = 8.31451\ J \cdot K^{-1} \cdot mol^{-1}$; $\Phi_m^\circ \overset{def}{=} \Delta_0^T S_m^\circ - \Delta_0^T H_m^\circ/T\}$

$\frac{T}{K}$	$\frac{C_{p,m}}{R}$	$\frac{\Delta_0^T S_m^\circ}{R}$	$\frac{\Delta_0^T H_m^\circ}{R \cdot K}$	$\frac{\Phi_m^\circ}{R}$	$\frac{T}{K}$	$\frac{C_{p,m}}{R}$	$\frac{\Delta_0^T S_m^\circ}{R}$	$\frac{\Delta_0^T H_m^\circ}{R \cdot K}$	$\frac{\Phi_m^\circ}{R}$
5	(0.017)	(0.0010)	(0.0031)	(0.0004)	280	8.116	7.710	1247.8	3.254
10	0.0088	0.0039	0.0261	0.0013	290	8.245	7.997	1329.3	3.413
15	0.0260	0.0102	0.1065	0.0031	300	8.363	8.278	1412.4	3.570
20	0.0560	0.0214	0.3045	0.0062	310	8.458	8.554	1496.5	3.727
25	0.1080	0.0389	0.7025	0.0108	320	8.528	8.824	1581.4	3.882
30	0.1950	0.0659	1.448	0.0176	330	8.588	9.087	1667.0	4.036
35	0.3180	0.1047	2.716	0.0271	340	8.643	9.344	1753.2	4.188
40	0.4760	0.1570	4.685	0.0399	350	8.700	9.596	1839.9	4.339
45	0.6610	0.2236	7.520	0.0564	375	8.818	10.20	2058.9	4.710
50	0.8660	0.3052	11.41	0.0771	400	8.910	10.77	2280.5	5.071
55	1.098	0.3983	16.30	0.1019	425	8.983	11.32	2504.3	5.423
60	1.337	0.5039	22.38	0.1309	450	9.045	11.83	2729.6	5.764
65	1.586	0.6208	29.69	0.1640	475	9.090	12.32	2956.4	6.097
70	1.834	0.7473	38.24	0.2011	500	9.111	12.79	3184.0	6.420
75	2.087	0.8824	48.04	0.2420	525	9.140	13.23	3412.1	6.734
80	2.338	1.025	59.10	0.2864	550	9.162	13.66	3640.9	7.039
85	2.591	1.175	71.43	0.3342	575	9.184	14.07	3870.2	7.336
90	2.844	1.330	85.02	0.3852	600	9.218	14.46	4100.2	7.625
95	3.088	1.490	99.85	0.4391	625	9.240	14.83	4331.0	7.906
100	3.358	1.655	115.9	0.4957	650	9.263	15.20	4562.2	8.180
105	3.593	1.825	133.3	0.5550	675	9.293	15.55	4794.2	8.446
110	3.818	1.997	151.8	0.6166	700	9.321	15.89	5026.9	8.706
115	4.042	2.172	171.5	0.6804	725	9.355	16.22	5260.3	8.960
120	4.266	2.348	192.3	0.7462	750	9.382	16.53	5494.5	9.207
125	4.487	2.527	214.1	0.8138	775	9.408	17.84	5729.4	9.448
130	4.690	2.707	237.1	0.8832	800	9.432	17.14	5964.9	9.684
135	4.881	2.888	261.0	0.9541	825	9.462	17.43	6201.1	9.914
140	5.062	3.068	285.9	1.026	850	9.482	17.71	6437.9	10.14
145	5.242	3.249	311.6	1.100	875	9.510	17.99	6675.3	10.36
150	5.415	3.430	338.3	1.175	900	9.539	18.26	6913.4	10.58
155	5.576	3.610	365.8	1.250	925	9.561	18.52	7152.1	10.79
160	5.734	3.789	394.0	1.327	950	9.583	18.77	7391.4	10.99
165	5.893	3.968	423.1	1.404	975	9.617	19.02	7631.4	11.20
170	6.050	4.147	453.0	1.482	1000	9.646	19.27	7872.2	11.40
175	6.205	4.324	483.6	1.561	1025	9.668	19.51	8113.7	11.59
180	6.344	4.501	515.0	1.640	1050	9.697	19.74	8355.7	11.78
190	6.596	4.851	579.7	1.800	1075	9.720	19.98	8598.4	11.97
200	6.811	5.195	646.8	1.961	1100	9.753	20.19	8841.8	12.15
210	7.011	5.532	715.9	2.123	1125	9.775	20.41	9085.9	12.33
220	7.203	5.863	787.0	2.286	1150	9.807	20.63	9330.7	12.51
230	7.374	6.187	859.9	2.448	1175	9.820	20.63	9330.7	12.51
240	7.535	6.504	934.4	2.611	1200	9.860	21.04	9822.1	12.86
250	7.695	6.815	1010.6	2.773					
260	7.836	7.119	1088.2	2.934	298.15	8.344 ±	8.23 ±	1396.9 ±	3.541 ±
270	7.977	7.418	1167.3	3.094		0.014	0.02	2.1	0.004

Experimental $C_{p,m}$ results over any part of the temperature range reported in this paper are unavailable in the literature for direct comparison. See section 4 below for a comparison of our results at $T \leqslant 340$ K with those reported in the literature at higher temperatures.

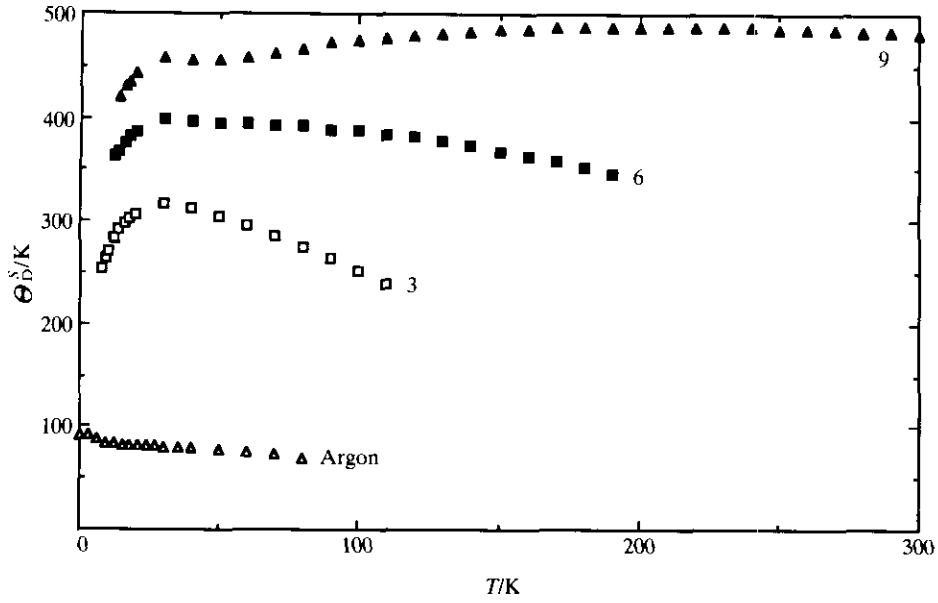

FIGURE 2. Plots of the Debye temperature Θ_D^S against temperature T for different numbers of vibrational modes per molecule as shown for $WSi_{2.06}$; that for Argon is also shown for comparison.

4. Analysis and discussion

THE DEBYE CHARACTERISTIC TEMPERATURE $\Theta_D(T)$

When the Debye model is obeyed, $\Theta_D(T)$ should be constant for any crystal. However, for real crystals, this model does not normally describe the experimental observations. In many diatomic lattices and metals. Θ_D asymptotically approaches constant values at high and low temperatures and shows a minimum in Θ_D at lower temperatures between the two extremes.[24]

The Debye temperature derived from the entropy $\Theta_D^S(T)$ for Ar(cr)[25,26] is a simple reference with which to compare WSi_2 (see figure 2). The decrease in Θ_D^S for Ar at $T \geqslant 20$ K is due mainly to the expansion of the lattice. For Ar, there is no ambiguity in the choice of the number of vibrations used in the calculation of Θ_D^S, namely three vibrations (translations) per molecule. On the other hand, when the lattice of a crystal is considered, the choice of the number of vibrations depends on which vibrations are excited in a particular range of temperature. The shape of the $\Theta_D(T)$ against T curve for molecular crystals, when calculated on the basis of three modes per molecule, will differ from that of Ar. Advantage can be taken of this to obtain qualitative information about the form of the frequency spectrum by varying the size of the vibrating unit and then examining the curves of $\Theta_D(T)$ against T in the different temperature regions.

The Θ_D^S for WSi_2, calculated using the Debye model, is plotted in figure 2 based upon three conditions of vibration: three, six, and nine modes. Θ_D^S was selected over Θ_D^C because it is less sensitive to errors in heat-capacity, which is especially important

at higher temperatures in view of our inability to make $(C_{p,m}-C_{V,m})$ corrections, as noted below. In figure 2, $\Theta_D^S(T)$ for three vibrations in WSi_2 rises rapidly from $T=3$ K and gradually flattens to a constant value over the narrow range $29<(T/K)<32$, implying that in this range the three modes of translation become fully excited in their contribution to the heat capacity. At $T>32$ K, the decline in the curve is due to the additional modes starting to contribute their energy to the heat capacity and to expansion of the WSi_2 lattice. It is this latter feature that accounts for the drop in $\Theta_D^S(T)$ for Ar. The $\Theta_D^S(T)$ for the curve for six modes in WSi_2 begins to flatten at $T=50$ K as the three librational modes become excited. At $T\geqslant 75$ K, this $\Theta_D^S(T)$ falls off as other contributions become active and the lattice expands further. Clearly, the translational and librational branches of the frequency spectrum are separated in WSi_2. At $T\geqslant 170$ K, the $\Theta_D^S(T)$ for nine modes reaches a constant value as the internal vibrational modes become fully excited. As the temperature rises above 240 K, the lattice continues to expand and the $(C_{p,m}-C_{V,m})$ corrections become significant.

It is evident from figure 2 that the drop in Θ_D^S at $T<20$ K for all the WSi_2 curves makes a reliable extrapolation to obtain $\Theta_D^S(T\rightarrow 0)$ virtually impossible. Such a drop results from the failure of the Debye model to account for our heat-capacity measurements.

TEMPERATURE DEPENDENCE OF $C_{p,m}$ AT TEMPERATURES BELOW 20 K

The failure of the Debye model at $T<20$ K noted above implies a possible contribution to the $C_{p,m}$ from a source other than the lattice vibrations. The fact that WTe_2 is known to be a conductor with interesting electrical properties[27,28] suggests that for WSi_2 an electronic term γT should be incorporated along with those representing the phonons.

The quantity measured calorimetrically is C_{sat}, the heat capacity of the solid in equilibrium with the saturated vapour Si(g), where p(Si) is miniscule. The background heat capacities of the vessel and helium exchange gas have been deducted from this quantity. A complete analysis of heat-capacity results over a wide temperature range requires $C_{V,m}$, which is related to $C_{sat,m}$ by

$$C_{sat,m}-C_{p,m}=(\partial p/\partial T)_{sat}\{(\partial H_m/\partial p)_T-V_m\}, \tag{1}$$

$$C_{p,m}-C_{V,m}=\alpha^2 V_m T/\kappa_T, \tag{2}$$

where $\alpha=V_m^{-1}(\partial V_m/\partial T)_p$ is the isobaric expansivity, V_m is the molar volume, and $\kappa_T=-V_m^{-1}(\partial V_m/\partial p)_T$ is the isothermal compressibility. The vapour pressure over solid WSi_2 is negligible so that $C_{sat,m}=C_{p,m}$ from equation (1). It should be noted that the pressure effect of the helium exchange gas ($p=2.0$ kPa at $T=20$ K) on the heat capacity of solid WSi_2: $(\partial C_{p,m}/\partial p)_T$, is also negligible. Returning to equation (2), low-temperature values of α, V_m, and κ_T are unavailable for WSi_2 but, fortunately, at the lowest temperatures in most solids, $(C_{p,m}-C_{V,m})$ becomes negligibly small.[29-31] Therefore, we have assumed that $C_{p,m}=C_{V,m}$ in the low-temperature region where our analysis is focused.

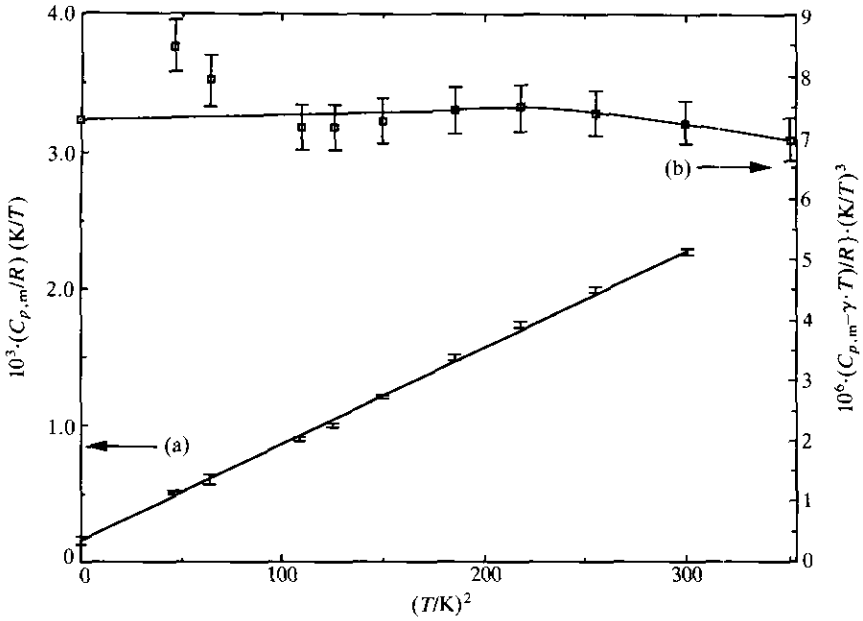

FIGURE 3. Plots of: (a), $C_{p,m}/RT$ and (b), $(C_{p,m}-\gamma T)/RT^3$ against T^2 for $WSi_{2.06}$. I, The vertical error bars correspond to: (a), $20(C_{p,m}/R)(K/T)$ and (b), $20\{(C_{p,m}-\gamma T)/R\}(K/T)^3$.

The heat capacity at very low temperature can be described by a power series of the form:

$$C_{V,m} = \gamma T + aT^3 + bT^5 + cT^7 + \cdots, \tag{3}$$

in which the coefficient γ arises from conduction of the electrons through the lattice[32] and the coefficients a, b, and c are related directly to the coefficients in the corresponding power series for the frequency spectrum at low frequencies.[33] As $T \rightarrow 0$, the lattice heat-capacity of the solid should equal that of an elastic continuum and is described by the Debye T^3 law: $C_{V,m} = aT^3$ and $\Theta_D^C = (12\pi^4 Nk/5a)^{1/3}$. The Θ_D^C is the Debye characteristic temperature derived from heat-capacity results rather than from the entropy.

A plot of $C_{p,m}/T$ against T^2 yields as $T \rightarrow 0$ the electronic γ as the intercept and the coefficient a of the first lattice term as the slope. From figure 3, the resulting $\gamma = (0.000160 \pm 0.000030)\, R \cdot K^{-1}$ or $(1.33 \pm 0.25)\, mJ \cdot K^{-2} \cdot mol^{-1}$ and $a = 10^{-4} \cdot (0.606 \pm 0.018)\, J \cdot K^{-4} \cdot mol^{-1}$. As a check on the determination of a, the plot of $(C_{p,m}-\gamma T)/T^3$ against T^2 (see figure 3) yielded when $T^2 \rightarrow 0$ an identical $a = 10^{-4} \cdot (0.606 \pm 0.019)\, J \cdot K^{-4} \cdot mol^{-1}$ as the intercept and the coefficient of the second lattice term $b = 10^{-10} \cdot (7.85 \pm 11.57)\, J \cdot K^{-6} \cdot mol^{-1}$ as the slope. Using this value of a in equation (3), $\Theta_D^C(T \rightarrow 0) = (317.8 \pm 3.3)$ K, which compares with 93.5 K for Ar.

Published values of the electronic molar heat capacity for related materials are scarce. For $MoSe_2$ and $MoTe_2$, $\gamma = 0$,[34] but for WTe_2 $\gamma = 5{\cdot}99\ mJ \cdot K^{-2} \cdot mol^{-1}$,[35] for WS_2 $\gamma = 3.6\ mJ \cdot K^{-2} \cdot mol^{-1}$,[36] and for $WC_{1.01}$ $\gamma = 0.79\ mJ \cdot K^{-2} \cdot mol^{-1}$.[37]

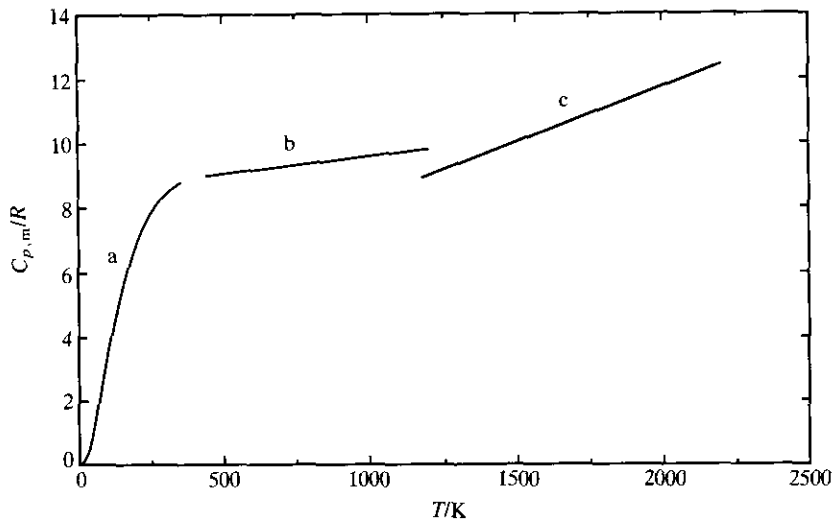

FIGURE 4. Experimental molar heat capacities $C_{p,m}$ at constant pressure plotted against temperature T for $WSi_{2.06}$ up to $T = 2200$ K: a, this work; b, Mezaki *et al.*;[10] c, Bondarenko *et al.*[11]

Our value of $1.33\ mJ \cdot K^{-1} \cdot mol^{-1}$ for $WSi_{2.06}$ compares with $1.3\ mJ \cdot K^{-2} \cdot mol^{-1}$ for pure tungsten.[38]

The low-temperature heat capacity of $WSi_{2.06}$ reported in this work has led to a reliable determination of its standard molar entropy: $S^{\circ}_{m}(WSi_{2.06}, cr, 298.15\ K) = (68.43 \pm 0.17)\ J \cdot K^{-1} \cdot mol^{-1}$. Together with its standard molar enthalpy of formation at $T = 298.15$ K recently reported by O'Hare[12] as $-(80.4 \pm 4.7)\ kJ \cdot mol^{-1}$, the standard molar entropies at $T = 298.15$ K for W[39,40] as $(32.66 \pm 0.2)\ J \cdot K^{-1} \cdot mol^{-1}$ and for Si[41] as $(18.820 \pm 0.2)\ J \cdot K^{-1} \cdot mol^{-1}$, the standard molar Gibbs free energy of formation is calculated to be $\Delta_f G^{\circ}_{m}(WSi_{2.06}, cr, 298.15\ K) = -(79.5 \pm 5.5)\ kJ \cdot mol^{-1}$. This compares with $-(91.9 \pm 9)\ kJ \cdot mol^{-1}$ from the Knudsen-effusion studies of Chart,[7] the uncertainty of which was criticized and revised by Chandrasekharaiah *et al.*[42] to $-(91.9 \pm 20)\ kJ \cdot mol^{-1}$, and the estimate by O'Hare:[12] $-(80 \pm 5)\ kJ \cdot mol^{-1}$.

MOLAR HEAT CAPACITY AT TEMPERATURES ABOVE 340 K

Enthalpy increments for WSi_2 were determined by Mezaki *et al.*[10] using drop calorimetry over the temperature range $461 \leqslant (T/K) \leqslant 1068$ from which $C_{p,m}$ values were derived as

$$C_{p,m} = \{8.576 + 10.7 \cdot 10^{-4} \cdot (T/K)\} \cdot R. \quad (4)$$

Their extrapolation at $T < 461$ K yielded $C_{p,m} = 8.897 \cdot R$ at $T = 300$ K, which lies above the value of $8.363 \cdot R$ of this work. A plot of their $C_{p,m}$ results against temperature using equation (4) permitted an extrapolation at $T < 460$ K to join our results smoothly at $T = 340$ K as shown in figure 4. The reproducibility of the $C_{p,m}$

results of Mezaki *et al.* is no better than $10^{-2} \cdot C_{p,m}$ and the uncertainty may be about $4 \cdot 10^{-2} \cdot C_{p,m}$, since their material was of industrial grade and was used without further purification. Nevertheless, the smooth connection of their heat capacities with those of this work justify their inclusion and preparation of thermodynamic functions up to $T = 1200$ K, which are given in table 2.

Heat-capacity results for WSi_2 derived from drop calorimetry have also been reported by Bondarenko *et al.*[11] but over the temperature range $1173 \leqslant (T/\mathrm{K}) \leqslant 2113$. The results from their equation:

$$C_{p,m} = \{4.125 + 37.094 \cdot 10^{-4}(T/\mathrm{K}) + 7.0527 \cdot 10^{5}(\mathrm{K}/T)^2\} \cdot R, \quad (5)$$

are also plotted in our figure 4 where it is evident that the curve defined by their $C_{p,m}$ values does not join smoothly with either the curves defined by Mezaki *et al.*[10] at $T < 1200$ K or with the results of this work at $T < 350$ K. Therefore, the thermodynamic functions listed in table 2 are not extended to $T > 1200$ K.

REFERENCES

1. Nicolet, M. A.; Lau, S. S. *VLSI Electronics: Microstructure Science*. Einspruch, N. G.; Larrabee, G. B.: editors. Academic Press: New York. **1983.** Vol. 6, p. 329.
2. Schlesinger, M. E. *Chem. Rev.* **1990,** 90, 607 and references therein.
3. Lehrer, W. I.; Pierce, J. M. *Proc. Electrochem. Soc.* **1981,** 81-5, 588.
4. Retajczyk, T. F.; Sinha, A. K. *Thin Solid Films* **1980,** 70, 241.
5. Biryukov, E. P.; Dostanko, A. P.; Mal'tsev, A. A.; Shakhlevich, G. M. *Phys. Chem. Mech. Surfaces* **1985,** 3, 1775.
6. Chart, T. G. *High Temp.-High Pressure* **1973,** 5, 241.
7. Chart, T. G. *Met. Sci.* **1975,** 9, 504.
8. Brewer, L.; Krikorian, O. *J. Electrochem. Soc.* **1956,** 103, 38.
9. Niessen, A. K.; Boer, F. R. de *J. Less Common Met.* **1981,** 82, 75.
10. Mezaki, R.; Tilleux, E. W.; Jambois, T. F.; Margrave, J. L. *Advances in Thermophysical Properties at Extreme Temperature and Pressure*. Gratch, S.: editor. ASME: New York. **1965,** p. 138.
11. Bondarenko, V. P.; Zmii, V. I.; Fomichev, E. N. *Poroshk. Metall.* **1972,** 12(2), 59.
12. O'Hare, P. A. G. *J. Chem. Thermodynamics* **1992,** 24, 1323.
13. Zachariasen, W. H. *Z. Phys. Chem. (Leipzig)* **1927,** 128, 39.
14. Kyono, I.; Sugano, M.; Nagase, R.; Hosaka, K.; Kato, A. *Jpn. Kokai Tokkyo Koho* JP 62,171,911. see *Chem. Abstr.* **1987,** 107, 157691b.
15. Westrum, E. F., Jr.; Furukawa, G. T.; McCullough, J. P. *Experimental Thermodynamics, Vol. 1*. McCullough, J. P.; Scott, D. W.: editors. Butterworths: London. **1968,** p. 133.
16. Stimson, H. F. *J. Res. Natl. Bur. Stand.* **1961,** 65A, 139.
17. McCrackin, F. L.; Chang, S. S. *Rev. Sci. Instrum.* **1975,** 46, 550.
18. Chirico, R. D.; Westrum, E. F., Jr. *J. Chem. Thermodynamics* **1980,** 12, 311.
19. Goldberg, R. N.; Weir, R. D. *Pure Appl. Chem.* **1992,** 64, 1545.
20. Bedford, R. E.; Durieux, M.; Muijlwijk, R.; Barber, C. R. *Metrologia* **1969,** 5, 47.
21. Westrum, E. F., Jr. *Proceedings NATO Advanced Study Institute on Thermochemistry at Viana do Castello, Portugal*. Ribeirio da Silva, M. A. V.: editor. Reidel: New York. **1984,** p. 745.
22. Andrews, J. T. S.; Norton, P. A.; Westrum, E. F., Jr. *J. Chem. Thermodynamics* **1978,** 10, 949.
23. *Pure and Appl. Chem.* **1986,** 58, 1678.
24. Blackman, M. *Handb. Phys.* **1955,** 7, 325.
25. Flubacher, P.; Leadbetter, A. J.; Morrison, J. A. *Proc. Phys. Soc. London* **1961,** 78, 1449.
26. Beaumont, R. H.; Chihara, H.; Morrison, J. A. *Proc. Phys. Soc. London* **1961,** 78, 1462.
27. Dawson, W. G.; Bullett, D. W. *J. Phys. C: Solid State Phys.* **1987,** 20, 6159.
28. Kabashima, S. *J. Phys. Soc. Jpn.* **1966,** 21, 945.
29. Mountfield, K. R.; Weir, R. D. *J. Chem. Phys.* **1976,** 64, 1768.
30. Brown, R. J. C.; Callanan, J. E.; Weir, R. D.; Westrum, E. F., Jr. *J. Chem. Phys.* **1986,** 85, 5963.
31. Brown, R. J. C.; Callanan, J. E.; Weir, R. D.; Westrum, E. F., Jr. *J. Chem. Thermodynamics* **1987,** 19, 1173.

32. Rosenburg, H. M. *Low Temperature Solid State Physics*. Oxford: Oxford University Press. **1963.**
33. Barron, T. H. K.; Berg, W. T.; Morrison, J. A. *Proc. Roy. Soc. London* **1957,** A242, 478.
34. Kiwia, H. L.; Westrum, E. F., Jr. *J. Chem. Thermodynamics* **1975,** 7, 683.
35. Callanan, J. E.; Hope, G. A.; Weir, R. D.; Westrum, E. F., Jr. *J. Chem. Thermodynamics* **1992,** 24, 627.
36. O'Hare, P. A. G.; Hubbard, W. N.; Johnson, G. K.; Flotow, H. E. *J. Chem. Thermodynamics* **1984,** 16, 45.
37. Chang, Y. A.; Toth, L. E.; Tyan, Y. S. *Met. Trans.* **1971,** 2, 315.
38. Cezairliyan, A.; Miller, A. P. *Specific Heat of Solids: Data Series on Material Properties, Vol. I-2*. Ho, C. Y.: editor. Hemisphere: London. **1988,** p. 39.
39. Clusius, K.; Franzosini, P. *Z. Naturforsch.* **1959,** 14A, 99.
40. Chase, M. W., Jr.; Davies, C. A.; Downey, J. R., Jr.; Frurip, D. J.; McDonald, R. A.; Syverud, A. N. *J. Phys. Chem. Ref. Data* **1985,** 14, Suppl. 1, pp. 1834, 1796.
41. Flubacher, P.; Leadbetter, A. J.; Morrison, J. A. *Phil. Mag.* **1959,** 4, 275.
42. Chandrasekharaiah, M. S.; Margrave, J. L.; O'Hare, P. A. G. *J. Phys. Chem. Ref. Data* (in the press).